



# Effect of a novel quaternary ammonium silane cavity disinfectant on cariogenic biofilm formation

U. Daood<sup>1</sup> · M. F. Burrow<sup>2</sup> · C. K. Y. Yiu<sup>3</sup>

Received: 2 October 2018 / Accepted: 30 April 2019  
© Springer-Verlag GmbH Germany, part of Springer Nature 2019

## Abstract

**Objective** Evaluate effect of quaternary ammonium silane (QAS) cavity disinfectant on cariogenic biofilm.

**Materials and methods** Single- (*Streptococcus mutans* or *Lactobacillus acidophilus*), dual- (*Streptococcus mutans*/*Lactobacillus acidophilus*), and multi-species (*Streptococcus mutans*, *Actinomyces naeslundii*, and *Streptococcus sanguis*) biofilms were grown on acid-etched dentine discs. Biofilms were incubated (120 min/37 °C) and allowed to grow for 3 days anaerobically. Discs (no treatment) served as control (group 1). Groups II, III, IV, and V were then treated with 2% chlorhexidine, and 2%, 5%, and 10% QAS (20 s). Discs were returned to well plates with 300 µL of bacterial suspension and placed in anaerobic incubator at 37 °C and biofilms redeveloped for 4 days. Confocal microscopy, Raman, CFU, and MTT assay were performed.

**Results** Raman peaks show shifts at 1450 cm<sup>-1</sup>, 1453 cm<sup>-1</sup>, 1457 cm<sup>-1</sup>, 1460 cm<sup>-1</sup>, and 1462 cm<sup>-1</sup> for control, 2% CHX, 2%, 5%, and 10% QAS groups in multi-species biofilms. There was reduction of 484 cm<sup>-1</sup> band in 10% QAS group. CLSM revealed densely clustered green colonies in control group and red confluent QAS-treated biofilms with significantly lower log CFU for single/dual species. Metabolic activities of *Streptococcus mutans* and *Lactobacillus acidophilus* decreased with increasing QAS exposure time.

**Conclusion** Quaternary ammonium silanes possess antimicrobial activities and inhibit growth of cariogenic biofilms.

**Clinical significance** Available data demonstrated use of QAS as potential antibacterial cavity disinfectant in adhesive dentistry. Experimental QAS can effectively eliminate caries-forming bacteria, when used inside a prepared cavity, and can definitely overcome problems associated with present available cavity disinfectants.

**Keywords** Raman · Dentine · Quaternary ammonium silane · *Streptococcus mutans* · CFU · Disinfectant

## Introduction

Incomplete removal of caries-infected dentine during cavity preparation may result in entrapment of bacteria within the cavity. These bacteria may remain with minimal nutrients to

survive; however, some biologically and chemically fit strains may dominate and establish beneath an already sealed restoration causing pulpal inflammation [1, 2]. *Streptococcus mutans*, responsible for recurrent caries initiation and development, is found beneath sealed restorations surviving at a low pH, as a result of acidogenesis of carbohydrates [3]. *Streptococcus mutans* is linked to caries due to its acidogenic and aciduric properties, contributing to extracellular matrix production construction and mutacin production [4]. This bacterium secretes enzymes that are part of the salivary pellicle synthesizing extra polysaccharide resulting in bacterial adhesion [5]. They are primary colonizers and facilitate co-aggregation and co-adhesion process serving as a substrate for other microorganisms leading to a large accumulation of biofilm maturation and microorganisms [6]. Following caries development, the population of the microflora may change from *Streptococcus mutans* to other non-mutant bacteria such as *Lactobacillus acidophilus* [7]. A strong correlation has been suggested between caries and the *Lactobacillus* count

✉ U. Daood  
umerdaood@imu.edu.my

<sup>1</sup> Clinical Dentistry, Restorative Division, Faculty of Dentistry, International Medical University Kuala Lumpur, 126, Jalan Jalil Perkasia 19, Bukit Jalil, Bukit Jalil, Wilayah Persekutuan, 57000 Kuala Lumpur, Malaysia

<sup>2</sup> Prosthodontic Dentistry, Faculty of Dentistry, The University of Hong Kong, Prince Philip Dental Hospital, 34 Hospital Road, Pokfulam, Hong Kong, SAR, China

<sup>3</sup> Paediatric Dentistry and Orthodontics, Faculty of Dentistry, The University of Hong Kong, Prince Philip Dental Hospital, 34 Hospital Road, Pokfulam, Hong Kong, SAR, China

[8]. *Lactobacillus* species found in dental caries cohabitate with other lactobacilli [9]. It is the ability of lactobacilli to ferment a variety of carbohydrates and survive in a relatively low pH environment making it extremely cariogenic [10]. It is the production of exopolysaccharides that is considered pivotal in the adherence of the biofilm structure [11]. These bacterial properties of both species define a major hallmark of caries process and a pivotal reason for using them in the study.

Dental composites are considered the most common alternative to dental amalgam. Cavities restored with moderate to large-sized composites are associated with high frequency of replacement or failures [12]. This is mainly due to in vivo biodegradation of the resin-dentine bonded interface, leading to loss of adhesion, microleakage, and recurrent caries [13]. Consequently with bacterial invasion along tooth-restoration margins, there is a major microbiological shift of the bonded interface from health to a disease-associated state [14]. Many antimicrobial compounds such as chlorhexidine (CHX), metal ions, bis-biguanides, and quaternary ammonium compounds have been used to reduce the effects of oral bacteria and inhibit recurrent caries [15]. Chlorhexidine digluconate has intense adsorption to the tooth structure along with strong antibacterial action [16]. Furthermore, it is known that application of low concentrations of CHX results in stability of the bonded interface by preventing degradation of the unprotected collagen fibrils in the hybrid layer from the host-derived MMPs and cysteine cathepsins [17, 18]. However, CHX can be displaced by competing cations from dentinal fluid and saliva, thereby compromising its antimicrobial and protease inhibitory effects over time [19].

Quaternary ammonium compounds have been used as disinfectants on unbroken skin, non-critical surfaces, and mucous membranes [20]. The organosilicon quaternary ammonium compounds (3-(trimethoxysilyl)-propyldimethyloctadecyl ammonium chloride) (SiQAC;  $C_{26}H_{58}ClNO_3Si$ ; CAS Registry Number 27668-52-6) are cationic and have a quaternary ammonium end group with reactivity of carbon-silicon bonds [21]. The hydrolysis products of SiQAC exhibited antimicrobial activities against a broad range of microorganisms, while chemically bonded to a variety of surfaces [22]. These compounds exert a strong positive charge, inadvertently effecting the negatively charged cell wall of bacteria, resulting in inhibition of bacterial growth [23]. The principal targets for these compounds are the lipid bilayer hydrophobic interior of the bacterial membrane, which is interposed with the hydrocarbon cationic tail of the quaternary ammonium amphiphile [24]. Their long alkyl lipophilic chain (C18) is found to possess rapid antibacterial action and controlled degradation as a result of pH sensitivity of their hydrolysis [25].

The quaternary ammonium compounds, SiQAC, have been coupled with trialkoxysilanes with methacryloxy or epoxy functionalities via sol-gel platform chemistry that utilizes tetraethoxysilane (TEOS) or dimethyldiethoxysilane as the

anchoring unit, generating a host of quaternary ammonium silanes (QAS) molecules with antimicrobial activities [26, 27]. Recently, using similar platform chemistry, an ethanol- or acetone-soluble, fully hydrolyzed, partially condensed version of QAS (codenamed K21; CAS Registry Number 1566577-36-3; IUPAC name: 1-octadecanaminium, N,N'-[[[3,3-bis [[3-(dimethyloctadecylammonio)propyl]dihydroxysilyl]oxy]-1,1,5,5,-tetrahydroxy-1,5-trisiloxanediy]di-3,1-propanediyl] bis[N,N-dimethyl] chloride (1:4)) has been synthesized and safe for intraoral use as the hydrolysis by-product of the sol-gel reaction is ethanol. Being devoid of a methacryloxy functional group, the disinfectant can be used in cavities that are to be restored with resin composite, glass ionomer cement, or amalgam restorative materials. The application of cavity disinfectants and the removal of biofilms are important alternatives for caries control as they aim to reduce the spread of bacterial influx.

There are conservative approaches towards identification of bacteria in different conditions based on morphological evaluation [28]. Vibrational spectroscopic techniques such as Raman spectroscopy provide a long tradition of identifying vibrational spectra as an alternative approach by displaying finger prints of the chemical composition of bacteria and biofilm [29]. Therefore, this paradigmatic approach is employed in the present study to obtain the different spectra from a multi-species biofilm grown on demineralized dentine matrix following QAS disinfection. Thus, the objective of the present study was to evaluate the antimicrobial effect of different concentrations of QAS cavity disinfectants against both *Streptococcus mutans* and *Lactobacillus acidophilus* as single- and dual-species biofilms. In addition, Raman spectroscopy was performed on dentine substrates onto which multi-species biofilms (*Streptococcus mutans*, *Actinomyces naeslundii*, and *Streptococcus sanguis*) were grown and treated with QAS cavity disinfectants. Raman spectroscopy was performed to analyze the biofilm structure and changes within the demineralized dentine structure induced by biofilm and application of cavity disinfectants. The null hypotheses tested were that the QAS cavity disinfectants (i) had no antimicrobial effect on the single-species and dual-species biofilms, (ii) had no effect on the multi-species biofilm, and (iii) demineralized dentine collagen matrix.

## Materials and methods

One hundred forty-five sound human molars (from donors aged 21–34 years) were stored in chloramine T solution at 4 °C for no more than 3 months after extraction. The teeth were collected after the patient's informed consent was obtained under a protocol approved by the Institutional Review Board of the University of Hong Kong (UW14-406). Forty-five teeth were used for single- and dual-species biofilm ( $n = 3$ ) development for confocal laser scanning microscopy

(CLSM) and 45 teeth for colony-forming unit (CFU) analysis ( $n = 3$ ). Twenty-five teeth were used for multi-species biofilm development and micro-Raman analysis ( $n = 5$ ). A further 30 teeth were utilized for 3-[4,5-dimethylthiazol-2-yl]-2,5-diphenyltetrazolium bromide (MTT) assay ( $n = 3$ ).

## Drug

The QAS cavity disinfectant examined in the present study was synthesized by sol-gel reaction between 1 mol of TEOS (Mw 208) and 4 mol of Et-SiQAC (Mw 538) as reported previously by Daood et al. [30, 31]. Briefly, 1 mol of TEOS (Mw 208) and 4 mol of 3-(triethoxysilyl)-propyldimethyloctadecyl ammonium chloride (i.e., the ethoxy version of SiQAC, abbreviated as Et-SiQAC; Mw 538). In a typical synthesis, 2.08 g of TEOS was blended with 29.89 g of 3-(triethoxysilyl)-propyldimethyloctadecyl ammonium chloride (72% of Et-SiQAC dissolved in ethanol) and 5 mL of ethanol (to render the blend more homogeneous). Hydrolysis was initiated by the addition of 10.08 g of 0.02 M HCl-acidified water (pH 1.66, representing 3.5 times the stoichiometric molar concentration of water required, to ensure complete hydrolysis). Completion of the hydrolysis reaction (approximately 3 h) was indicated by the disappearance of absorbance peaks of the Si–O–C peak at  $1078\text{ cm}^{-1}$  and the  $\text{OC}_2\text{H}_5$  peak at  $1172\text{ cm}^{-1}$  [31].

## Dentine disc preparation

### Dentine disc preparation for single, dual-, and multi-species biofilms, CFU counts, and MTT analysis

Forty-five teeth were used for CLSM analysis of single- and dual-species biofilms following application of cavity disinfectants. The occlusal enamel was cut perpendicular to the long axis of the teeth with a low-speed diamond saw (Isomet, Buehler Ltd., Lake Bluff, IL, USA), exposing the mid coronal dentine 1 mm below the dentino-enamel junction using a water coolant. Three dentine discs of 1 mm thickness were prepared for triplicate analysis for each group ( $n = 3$ ). After examining the dentine discs under a stereomicroscope, specimens with cracks or lesions were removed. The dentine discs were wet-polished with 1200-grit SiC papers for surface standardization of the smear layer and rinsed with deionized water for 5 min under ultrasonic agitation. The polished surfaces were blot-dried using absorbent paper (Kimwipes; Kimberly Clark Corp, Roswell, GA, USA). The smear layer was removed from the dentine discs by treatment with 1% citric acid for 5 min and later rinsed with deionized water [32]. The dentine discs were sterilized by autoclaving at  $121\text{ }^\circ\text{C}$  for 15 min. The sterilized dentine discs were anchored vertically in a 24-well culture plate. Dentine discs ( $n = 3$ ) for CFU count and MTT assay were similarly prepared as for CLSM analysis

of single- and dual-species biofilms. Five discs were randomly selected for each group ( $n = 5$ ) to grow the multi-species biofilms for Raman spectroscopy analysis. Discs receiving no treatment served as the control.

## Preparation and growth of biofilms

### Bacterial strains 1. Single- and dual-species biofilms

*Streptococcus mutans* ATCC (American type culture collection) 35668 and *Lactobacillus acidophilus* ATCC 4356 were used for single- and dual-species biofilm formation. All bacteria were cultured on blood agar plates at  $37\text{ }^\circ\text{C}$  for 16 to 20 h anaerobically. Later, a distinct colony of each bacterium was transferred for further incubation. The single-colony species were cultured anaerobically in brain heart infusion (BHI) broth supplemented with 8% sucrose (pH 7.4) and a minimal amount of xylitol (0–2%) at  $37\text{ }^\circ\text{C}$  for 48 h. After the cells were harvested by centrifugation at 4000 rpm for 10 min, each of the cell pellets was washed three times with sterile phosphate-buffered solution (PBS, 0.01 M, pH 7.2), later re-suspended in 100 mL of respective growth medium and adjusted to a concentration of McFarland 3 ( $10^9$  cells/mL) before use.

### 2. Multi-species biofilms

*Streptococcus mutans* ATCC 35668, *Actinomyces naeslundii* ATCC 12104, and *Streptococcus sanguis* ATCC 10556 were used for multi-species biofilm formation. These microorganisms were previously associated with the ecological oral biofilm concept, as the organisms are well-characterized viridans group and better candidates to study as early colonizers in the mouth producing acids [33]. *Streptococcus mutans*, *Actinomyces naeslundii*, and *Streptococcus sanguis* were cultured separately anaerobically in BHI broth, which had been supplemented with 8% sucrose (pH 7.4) and a minimal amount of xylitol (0–2%) at  $37\text{ }^\circ\text{C}$  for 48 h. The low concentration of xylitol enhanced the chance of bacterial colonies to grow through their log phase. After the cells were harvested by centrifugation at 4000 rpm for 10 min, each of the cell pellets was washed three times with sterile PBS (0.01 M, pH 7.2) and later re-suspended in 100 mL of growth medium and adjusted to a concentration of McFarland 0.5 ( $10^7$  cells/mL) before use. For multi-species biofilms, the bacterial suspension was prepared and mixed to give the defined bacterial population ( $10^7$  CFU/mL).

## Harvesting of biofilms on dentine discs

### 1. Single- and dual-species biofilms

A 300  $\mu\text{L}$  aliquot of each bacterial culture was mixed and transferred to the dentine discs individually for single-colony

specimens, positioned in sterile 24-well tissue culture plates (Thermo Fisher Scientific Inc.) and incubated at 37 °C in an anaerobic chamber to allow bacterial adhesion for 3 days. Similarly, dual colonies of *Streptococcus mutans* and *Lactobacillus acidophilus* were incubated at a ratio of 60/40 respectively for each group. The lactobacilli are expected to have high counts and outgrow *Streptococcus mutans* [34]. The biofilms were first incubated for 120 min at 37 °C in an orbital shaker incubator at 75 rpm for assisting the adhesion phase. The biofilms ( $10^7$  CFU/mL) were allowed to grow for 3 days under anaerobic conditions (85% nitrogen, 10% hydrogen, and 5% carbon dioxide). The medium was replaced daily with a fresh solution and the pH of the culture media ( $7.4 \pm 0.2$ ) was determined every 24 h.

## 2. Multi-species biofilms

For multi-species biofilms on dentine, the autoclaved discs were transferred to a 12-well sterile tissue culture plate (Thermo Fisher Scientific Inc.) containing 2 mL of multi-species biofilm for each group ( $n = 3$ ), respectively, and incubated similarly as the single species for 120 min at 37 °C in an orbital shaker incubator at 50 rpm. The multi-species biofilms ( $10^7$  CFU/mL) were also grown for 3 days under anaerobic conditions (85% nitrogen, 10% hydrogen, and 5% carbon dioxide). The media was refreshed every day.

**Application of CHX and QAS cavity disinfectants** After 3 days of biofilm growth, group I dentine discs were not treated with any cavity disinfectant and served as a control. In groups II, III, IV, and V, the dentine surfaces were treated with 2% CHX, 2%, 5%, and 10% QAS, respectively, using a sterile saturated micro brush (Dentsply/DeTrey; Konstanz, Germany) for 20 s using a gentle dabbing motion, followed by a gentle blast of compressed air for 5 s. Care was taken not to disturb the dentine discs with in vitro grown biofilms. After treatment with the cavity disinfectants, the dentine discs were left for 20 s for evaporation of the solvent, returned to the well plates with 300  $\mu$ L of bacterial suspension immediately, and placed in the sterile incubator inside the anaerobic chamber at 37 °C. The microorganisms were allowed to redevelop for 4 more days before CLSM, CFU count, MTT assay, and Raman analysis.

## Raman data acquisition and processing

For Raman measurements, specimens were drawn after 7 days from culture plates and allowed to dry for 15 min at 35 °C. The dentine disc specimens were transferred to a low fluorescent quartz microscopic slide. Areas of approximately 10  $\mu$ m were chosen randomly across all dried biofilm disc specimens. A Raman spectroscope equipped with a Leica microscope and lenses (JY LabRam HR 800; Horiba Jobin Yvon, France) with curve-fitting Raman software (Labspec 5) was used for

analysis. Excitation was provided using micro-Raman parameters at zero calibration: 785 nm wavelength with argon ion 514.5 green laser excitation (better for organic/inorganic structures and has better sensitivities; to increase the signal to be analyzed), nm laser (spectral resolution of  $1.6 \text{ cm}^{-1}$ ), and power  $< 500 \text{ }\mu\text{W}$  at  $\times 100$  objective with a superior signal/noise ratio. To generate one spectrum of the biofilms, six frames of 30-s exposure were recorded and later subjected to system background removal, spectral analysis, and dark count correction with intensity normalized. All spectra were recalibrated to the amplitude of the spectrums presumed to also contribute from the bacterial colonies normalized to the peaks  $1450 \text{ cm}^{-1}$  ( $\text{CH}_2$  deformations),  $1655 \text{ cm}^{-1}$ ,  $1245 \text{ cm}^{-1}$ , and  $1070 \text{ cm}^{-1}$  wavenumber regions for biofilm changes. The spectral distance was also calculated using Origin 8.5 Pro Lab software. Little fluorescence was observed in the dried biofilm specimens due to the diameter of the laser used. The measurement was done on an automated  $x$ - $y$ - $z$ -axis-positioning stage, which held the dentine discs on a glass slide. The objective was used to visually identify the position for obtaining the Raman signals and precision of chemical data at different locations in the intertubular dentine of the disc specimens inducing the Raman scattering effect. Specimens of mineralized and non-mineralized dentine specimens with no biofilm grown were also analyzed for generation of standard spectra with an exposure time on each scan of 60 s in the information-rich region between 200 and  $3200 \text{ cm}^{-1}$  including the biofilm specimens. All spectra were obtained at room temperature and in the dark to avoid any spikes originating due to ambient light. The changes within the inorganic and organic dentine components were analyzed by comparing the Raman peaks centered at  $434 \text{ cm}^{-1}$  (stretching vibration of  $\text{V}_2\text{PO}_4$ ) [35] and  $960 \text{ cm}^{-1}$  (hydroxyapatite  $\text{PO}_4$ ) [36] for inorganic, and  $484 \text{ cm}^{-1}$  (polysaccharides or carbohydrates) [37],  $1655 \text{ cm}^{-1}$  (amide I {C=O}) [38], and  $1454 \text{ cm}^{-1}$  (pyrrolidine rings of proline and hydroxyproline inside collagen) [39] for organic to the peak at  $1070 \text{ cm}^{-1}$ .

## Confocal laser scanning microscopy

Following the secondary bacterial adhesion phase, the viability of bacteria in single- and dual-species biofilms on dentine was examined using CLSM (Fluoview FV 1000, Olympus, Tokyo, Japan). Live/Dead BacLight bacterial viability (molecular probe #L7012 LIVE/DEAD BacLight stain; Invitrogen) was used with green stains for viable bacteria, while red stains were damaged and dead bacteria (SYTO 9 live stain and 568 nm for PI dead stain). Live/dead bacteria were mixed according to the manufacturer's instructions. After 30 min of incubation in the dark, excessive stain was removed from the dentine discs using absorbent paper. The biofilm was imaged on a CLSM using light emission between 500 and 550 nm with an excitation wavelength of 488 nm and  $\times 100$  objective

lens for direct observation. Five images were taken from each biofilm specimen for examination using bioimageL software (v.2.0. Malmö, Sweden), which provides information on the structure of the biofilm including green- and red-stained bacteria volume on a two-dimensional  $x$ - $y$  section, based on color segmentation algorithms written in MATLAB. The respective percentages for live and dead bacteria for each group were calculated.

### CFU count

Growth kinetics of the single- and dual-species biofilms were assessed by quantifying bacterial counts in colony-forming units (CFU). Both single- and dual-species biofilms were grown for 3 days on dentine discs ( $n = 3$ ), then treated with cavity disinfectants; 2% CHX, 2%, 5%, and 10% QAS for 20 s and regrown for 4 days to complete a week cycle as mentioned previously. The biofilms from the dentine samples were collected in 1 mL of sterile BHI broth (pH 7.4) and incubated at 37 °C for 24 h. A 100  $\mu$ L of broth (each group separately) in 100  $\mu$ L of phosphate-buffered solution (PBS) inside Eppendorf tubes (plastibrand micro centrifuge Tube/Z334006; Sigma-Aldrich) was centrifuged five times inside a micro centrifuge (Centrifuge 5430 R; Eppendorf AG, Hamburg Germany). Five microliters of each serial diluted sample was plated on selective BHI agar plates and incubated for 24 h. The microbial colony-forming units [CFU/mL] were counted and converted to log CFU.

### MTT analysis

The MTT assay was used to measure the metabolic activity of biofilms. It is a colorimetric assay that measures the enzymatic reduction of MTT, a yellow tetrazole, to formazan. The single-colony bacterial cells, *Streptococcus mutans*, and *Lactobacillus acidophilus* were harvested for 3 days, treated with cavity disinfectants; 2% CHX, 2%, 5%, and 10% QAS for 20 s and regrown as described above. The dentine discs ( $n = 3$ ) were autoclaved and washed with sterile saline solution to remove any unattached bacterial cells. A 2  $\mu$ L sample of *Streptococcus mutans* and *Lactobacillus acidophilus* was placed in Eppendorf tubes with individual treated dentine discs as described above for 15, 30, and 60 min. The bacterial suspension from the tubes was transferred to a 96-well micro-titer plate for assessment of bacterial cell viability to cleave the classical tetrazolium salt (3-[4,5-dimethylthiazol-2-yl]-2,5-diphenyltetrazolium bromide) (MTT) to a formazan dye (Boehringer Mannheim Corp, Indianapolis, IN, US). The plates were incubated for 4 h at 37 °C after adding the MTT labeling agent. The solubilization agent provided by the manufacturer was added and incubated for 24 h. After the appearance of purplish black formazan color, the plate was read at 560 nm in an Elisa reader (Dynatech MR 700). A higher

absorbance is related to a higher formazan concentration, indicating a higher metabolic activity of the biofilms.

### Statistical analysis

All data are presented as mean  $\pm$  standard deviation and were analyzed using a statistical package (SigmaStat Version 20, SPSS, Chicago, IL, USA software). All data were assessed for a normal distribution using the Shapiro-Wilk test for normality ( $p > 0.05$ ). One-way analysis of variance followed by the Tukey post hoc multiple comparison test was used to evaluate the effect of cavity disinfectants on the percentages of live and dead bacteria as well as log CFU. Two-way ANOVA followed by the Tukey post hoc multiple comparison tests was used to evaluate the effect of cavity disinfectants and time on the MTT relative absorbance values. All statistical analysis used a 95% confidence limit, so that  $p$  values  $\geq 0.05$  were not considered statistically significant.

## Results

### Confocal laser scanning microscopy

Representative CLSM images of single-species and dual-species biofilms of *Streptococcus mutans* and *Lactobacillus acidophilus* grown on dentine discs following treatment with different cavity disinfectants are shown in Figs. 1, 2, and 3, respectively. The *Streptococcus mutans* (Fig. 1a) and *Lactobacillus acidophilus* (Fig. 2a) single-species biofilms as well as dual-species biofilms grown (Fig. 3a) in the BHI medium showed densely clustered green colonies with minimal areas of dead bacterial cells; however, the majority of the bacteria present in the single- and dual-species biofilms fluoresced red in the 5% and 10% QAS groups, indicating mostly dead cells (Figs. 1d, e, 2d, e, and 3d, e). The amount of live bacteria in both single- and dual-species biofilms decreased significantly with increasing concentration of QAS ( $p < 0.05$ ) (Table 1). The highest dead cell count was observed in the 10% QAS groups (Table 2). No significant difference in dead cell count was found among 2% CHX, 2% QAS, and 5% QAS groups.

### CFU counts

The mean and standard deviations of log CFU counts for single- and dual-species biofilms following treatment with cavity disinfectants are shown in Table 2. The log CFU was the highest in the control dentine specimens without cavity disinfectant treatment. For single-species *Streptococcus mutans* biofilm, no significant difference in log CFU counts was found among 2% CHX ( $4.74 \pm 0.13$ ), 2% QAS ( $4.08 \pm 0.15$ ), and 10% ( $3.96 \pm 0.43$ ) QAS groups. For single-species

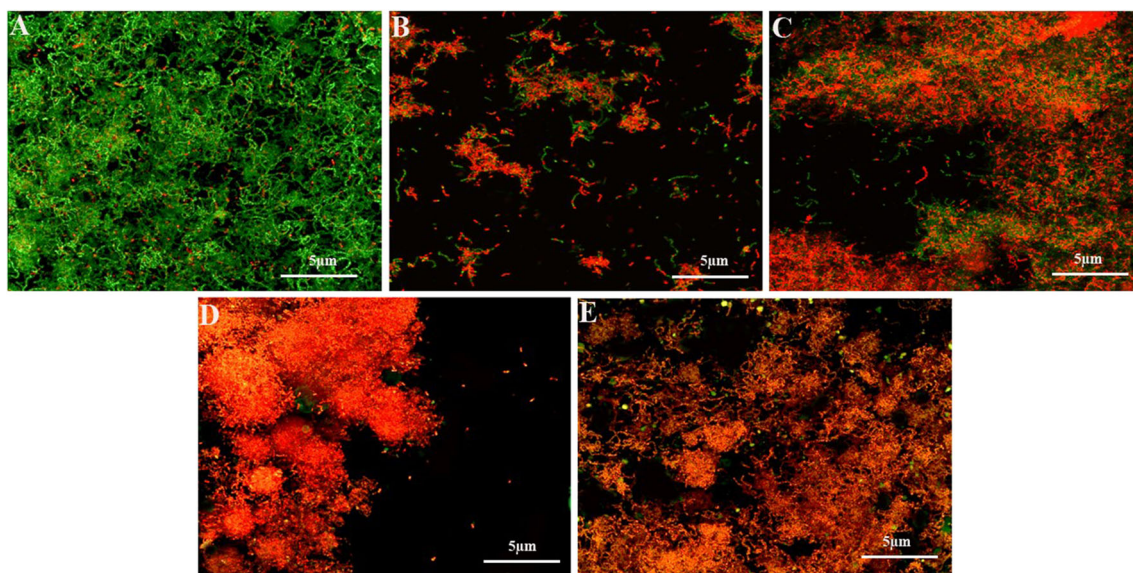


**Fig. 1** CLSM images of single-species *Streptococcus mutans* biofilm ( $\times 100$ ). Live bacterial cells appeared green, while dead cells appeared red. **a** Control. **b** 2% CHX. **c** 2% QAS. **d** 5% QAS. **e** 10% QAS

*Lactobacillus acidophilus* biofilm, no significant difference in log CFU counts was found among 2% CHX ( $3.41 \pm 1.17$ ), 2% ( $4.23 \pm 0.68$ ), 5% ( $4.80 \pm 0.70$ ), and 10% ( $3.79 \pm 0.39$ ) QAS groups. For *dual-species* biofilm, no significant difference in log CFU counts was found between 2% CHX ( $5.41 \pm 0.65$ ) and 2% QAS ( $4.68 \pm 0.76$ ) groups. Increasing the QAS concentration has no effect on the log CFU counts of the single- and dual-species biofilms.

### MTT

The viability of *Streptococcus mutans* and *Lactobacillus acidophilus* following treatment with cavity disinfectants

was assessed using MTT assay. The results are shown in Table 3. Results of two-way ANOVA showed that both factors, time ( $p < 0.05$ ) and cavity disinfectants ( $p < 0.05$ ), were significant and their interaction was also significant ( $p < 0.05$ ). The control dentine discs had biofilms with a high metabolic activity compared to the other four groups. The metabolic activity of *Streptococcus mutans* and *Lactobacillus acidophilus* biofilms decreased with increasing exposure time to cavity disinfectants. No significant difference in metabolic activity of *Streptococcus mutans* and *Lactobacillus acidophilus* biofilm was found between 2% CHX and 2% QAS after 60-min exposure. Increasing the concentration of QAS significantly

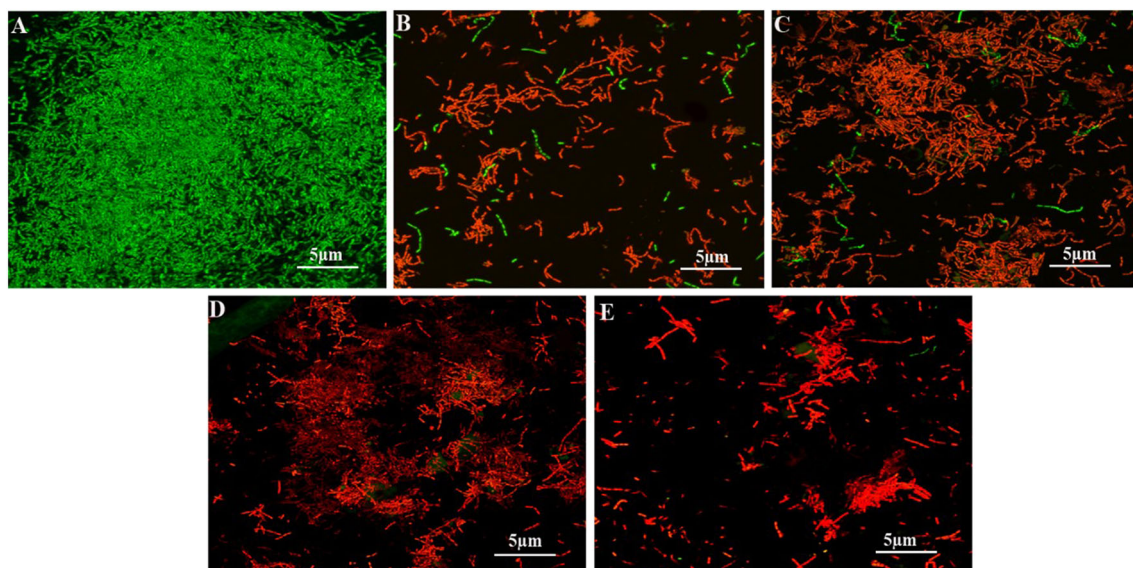


**Fig. 2** CLSM images of single-species *Lactobacillus acidophilus* biofilms ( $\times 100$ ). Live bacterial cells appeared green, while dead cells appeared red. **a** Control. **b** 2% CHX. **c** 2% QAS. **d** 5% QAS. **e** 10% QAS

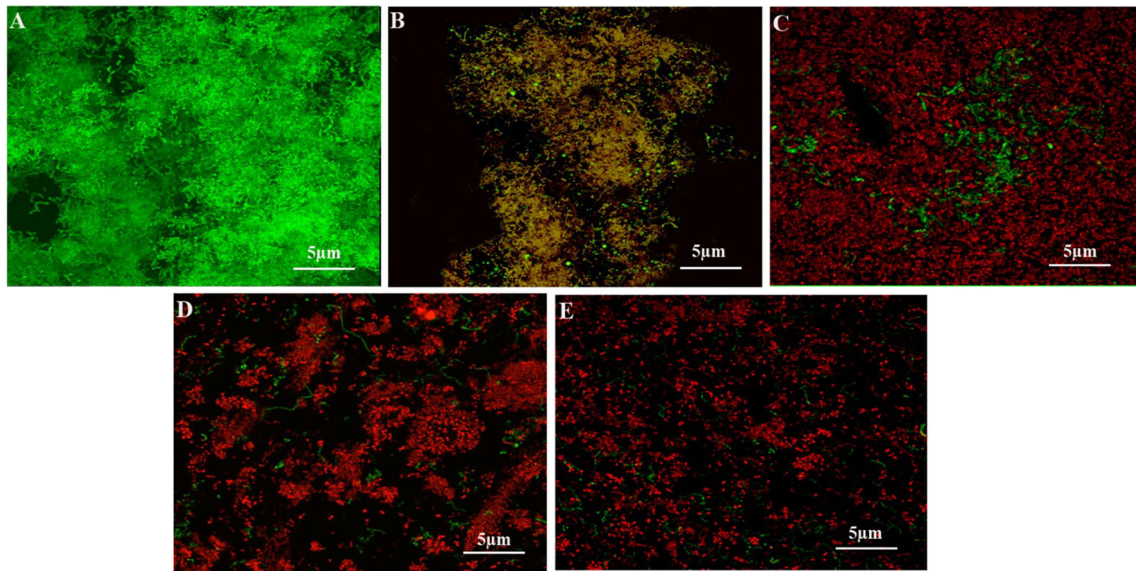


**Fig. 3** CLSM images of dual-species *Streptococcus mutans* and *Lactobacillus acidophilus* biofilms ( $\times 100$ ). Live bacterial cells appeared green, while dead cells appeared red. **a** Control. **b** 2% CHX. **c** 2% QAS. **d** 5% QAS. **e** 10% QAS

decreased metabolic activity of *Lactobacillus acidophilus* biofilm ( $p < 0.05$ ).

**Table 1** Bacterial viability in single- and dual-species biofilms following different cavity disinfectant treatments

	Dead		Live			
	Mean %	SD	Mean %	SD		
<i>S. mutans</i>						
Control	0.31	I	0.41	99.28	I_1	0.84
2% CHX	65.97	II	6.84	32.39	II_1	6.71
2% QAS	71.34	II	9.17	25.68	II_1	6.39
5% QAS	74.97	II	14.59	24.97	II_1	14.48
10% QAS	80.51	II	4.97	18.38	II_1	6.53
<i>L. acidophilus</i>						
Control	1.61	A	1.64	98.32	A1	1.67
2% CHX	61.95	B	12.71	36.11	B1	10.88
2% QAS	67.07	B, C	3.90	31.41	B1	3.29
5% QAS	72.70	B, C	5.71	31.16	B1	7.90
10% QAS	84.54	D	8.45	14.81	C1	8.59
<i>S. mutans</i> and <i>L. acidophilus</i>						
Control	2.33	a	2.02	97.67	b1	2.02
2% CHX	68.61	b	6.75	29.19	b1	4.96
2% QAS	71.18	b	2.48	27.54	b1	3.29
5% QAS	76.30	b, c	1.06	23.77	b1	1.23
10% QAS	83.99	c	1.73	15.33	c1	1.67

Values are means  $\pm$  standard deviation. Groups identified by different numerals and letters were significantly different at  $p < 0.05$

CHX chlorhexidine, QAS quaternary ammonium silane

### Raman data acquisition

Raman spectroscopy was carried out in the experiments with smears of modeled and established biofilms grown on demineralized dentine discs. It is well known that the half width peaks at  $1246\text{ cm}^{-1}$  (amide III) and  $1450\text{ cm}^{-1}$  (C–H alkyl group), result from  $\text{CH}_2\text{CH}_3$  asymmetric bend (rock), while the  $1667\text{ cm}^{-1}$  (amide I) corresponds to Raman scattering of the collagen [40, 41]. The molecules within the functional and the aromatic groups have delocalized electrons, which are easily polarized due to the presence of free electrons and double bonds, resulting in increased Raman shifts [42]. The low-power infrared laser used eliminated the sample fluorescence due to the rotation of molecules and transitions that are easily evaluated within the absorption and scattering spectral data.

### Biofilm changes

From the spectrum, it can be observed that the bands in this region respond mostly with treatment on the biofilm and typify changes within the absorbance spectrum with intensity increases with increasing QAS concentrations. Raman spectra showed signals detected in all samples with biofilm at  $484\text{ cm}^{-1}$  with more obvious variations in spectra from biofilm samples according to the disinfectants used (Fig. 4). The weak bands refer to the glycosidic link or the ring breath of possible polysaccharides within the biofilm or spectroscopic signature due to linkages of polysaccharides. There was a gradual reduction and striking difference of the  $484\text{ cm}^{-1}$  band as the concentration reaches 10% QAS.

**Table 2** Bacterial counts (log CFU) following different cavity disinfectant treatments

Disinfectant	<i>Streptococcus mutans</i>			<i>Lactobacillus acidophilus</i>			Dual-species		
	Log	SD		Log	SD		Log	SD	
Control	6.27	0.08	I	6.20	0.08	A	6.26	0.12	a
2% CHX	4.74	0.13	II	3.41	1.17	B	5.41	0.65	a, b
2% QAS	4.08	0.15	II, III	4.23	0.68	B	4.68	0.76	b, c
5% QAS	3.56	0.59	III	4.80	0.70	B	4	0.36	c
10% QAS	3.96	0.43	II, III	3.79	0.39	B	3.59	0.34	c

Values are means  $\pm$  standard deviation. Groups identified by different numerals and letters were significantly different at  $p < 0.05$

## Dentine substrate changes

Figure 5 shows the CH<sub>2</sub> (1450–1455 cm<sup>-1</sup>) bending region (dotted line) and changes in the intensities of the conventional spectral absorbance following treatment with different cavity disinfectants. The figure shows a correlation spectrum among all groups of the CH<sub>2</sub> bending region. Analysis of the peaks shows the respective changes: shifts at 1450 cm<sup>-1</sup>, 1453 cm<sup>-1</sup>, 1457 cm<sup>-1</sup>, 1460 cm<sup>-1</sup>, and 1462 cm<sup>-1</sup> for control, 2% CHX, 2% QAS, 5% QAS, and 10% QAS. The assignment of Raman bands for reference analysis is summarized in Table 4.

Deformation vibrations of single-bond stretch for amino acids (870 cm<sup>-1</sup> [43] and 1024 cm<sup>-1</sup> [44]) disappeared or displayed less signals and peaks in the 10% QAS-treated specimens compared to other specimens with C–C (1128 cm<sup>-1</sup>) [45] seen between 700 and 1200 cm<sup>-1</sup>. In particular, the Raman spectrum at amide III regions in the 2%, 5%, and 10% QAS groups showed maximum intensity compared to the control (Fig. 5). The amide I band (amide vibrations) at 1665 cm<sup>-1</sup> (not shown) was observed as a strong and broad band, particularly in the 2%, 5%, and 10% QAS-treated specimens. The shifts in amide I for control, 2% CHX, 2%, 5%, and 10% QAS specimens were 1665 cm<sup>-1</sup>, 1665 cm<sup>-1</sup>, 1658 cm<sup>-1</sup>, 1656 cm<sup>-1</sup>, and 1653 cm<sup>-1</sup>. The Raman spectra treated with 5% and 10% QAS revealed higher intensities and

an intense band around 1350 cm<sup>-1</sup> (arrows). A new broad isolated peak was found centered at 1130 cm<sup>-1</sup> in specimens treated with 5% QAS and a narrow peak in the control. There were deviations in the Raman spectrum at 1129–1130 cm<sup>-1</sup> C–C skeletal backbone with the representative spectra showing reduction in shifts: 1128 cm<sup>-1</sup>, 1128 cm<sup>-1</sup>, 1124 cm<sup>-1</sup>, 1121 cm<sup>-1</sup>, and 1119 cm<sup>-1</sup> respectively for control, 2% CHX, 2%, 5%, and 10% QAS (Table 4).

Moreover, the result was corroborated with the emergence of a peak at 1513–1515 cm<sup>-1</sup> in some of the specimens where the spectral peaks changed and became variable as the specimens were treated with different cavity disinfectants to well-formed peaks with peaks dominating in 5% and 10% QAS (Fig. 6). The peak may amount to amide II as it occurs in the vicinity of the 1515–1530 cm<sup>-1</sup> region.

## Discussion

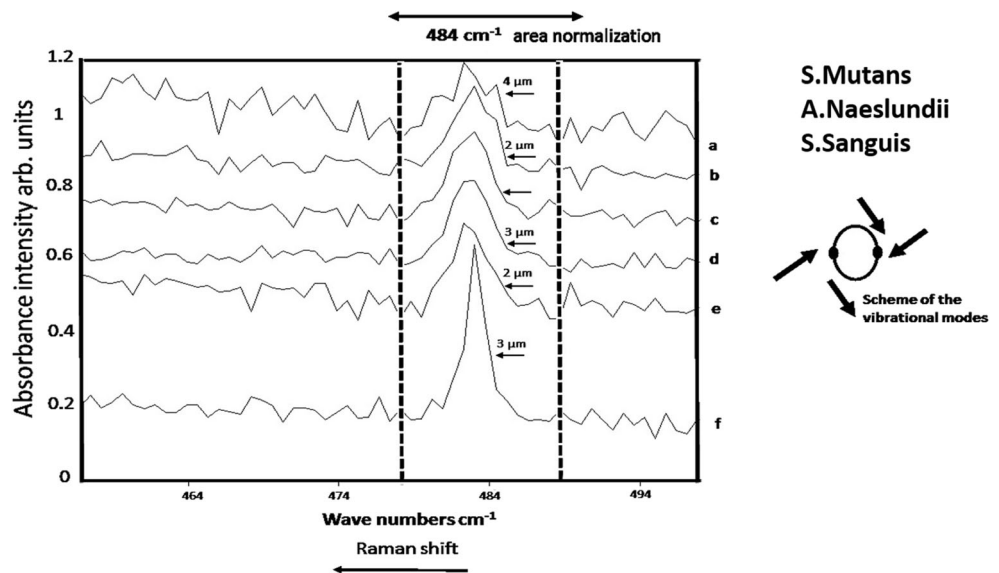
When using a minimally invasive operative caries management strategy, caries removal is often limited to the more superficial caries-infected dentine with partial removal of caries-affected dentine, and residual microorganisms may be left in the prepared tooth cavity, increasing the risk of pulpal inflammation and recurrent caries. Recurrent caries occurring

**Table 3** MTT metabolic activity following different cavity disinfectant treatments. Biofilms were grown for 15, 30, and 60 min

		15 min			30 min			60 min		Control		
		Mean	SD		Mean	SD		Mean	SD	+	-	
<i>Streptococcus mutans</i>	2% CHX	1.45	$\pm 0.46$	a	1.11	$\pm 0.10$	c	1.10	$\pm 0.20$	c	2.05	0.07
	2% QAS	1.31	$\pm 0.16$	b	1.13	$\pm 0.17$	c	0.95	$\pm 0.12$	c, d		
	5% QAS	1.10	$\pm 0.18$	c	0.83	$\pm 0.08$	c, d	0.546	$\pm 0.11$	d		
	10% QAS	1.14	$\pm 0.25$	b, c	0.88	$\pm 0.09$	c, d	0.35	$\pm 0.12$	d		
<i>Lactobacillus acidophilus</i>	2% CHX	2.27	$\pm 0.15$	A, B	2.45	$\pm 0.49$	A	1.75	$\pm 0.23$	D	3.20	0.08
	2% QAS	2.23	$\pm 0.18$	B	1.98	$\pm 0.19$	C, D	1.56	$\pm 0.22$	D, E		
	5% QAS	2.21	$\pm 0.10$	B, C	1.42	$\pm 0.17$	E	0.67	$\pm 0.13$	F		
	10% QAS	1.02	$\pm 1.02$	E, F	0.71	$\pm 0.20$	F	0.42	$\pm 0.11$	F		

Values are means  $\pm$  standard deviation. Groups identified by different superscripts were significantly different at  $p < 0.05$ .

**Fig. 4** Raman spectra of multi-species biofilms grown on demineralized dentine specimens and treated with different concentrations of QAS and CHX disinfectants. Spectral differences of control and treated specimens can be seen in the  $484\text{ cm}^{-1}$  region after normalization: (a) 10% QAS, (b) 5% QAS, (c-d) 2% QAS; (e) 2% CHX; (f) Control



at the resin-dentine interface has been the foremost reason for replacement of dental composite restorations [46] with *Streptococcus mutans* being the core bacterial microorganism responsible for recurrent decay [47]. Therefore, there is a need for the use of cavity disinfectants prior to the placement of non-antimicrobial restorative materials to eliminate residual bacteria, prevent bacterial growth, and invasion of the bonded interfaces.

This study provides important information on the antimicrobial effects of QAS on the single- and dual-species biofilms. The QAS cavity disinfectants are used to remove residual microorganisms prior to placement of the bonded

restorations. Results from CLSM and CFU have shown that QAS has a significant antimicrobial effect against both *Streptococcus mutans* and *Lactobacillus acidophilus* biofilms, which are the two most important bacteria associated with dentine caries. *Streptococcus mutans* is the most predominant bacteria related to primary and recurrent caries, which exemplifies the cariogenic properties of sucrose metabolism, acidogenity via fermentation, adherence, and biofilm formation via synthesis of extracellular glucans [48]. *Lactobacilli* are regarded as a major contributor to caries progression and the ability of *Lactobacilli* to form a biofilm was significantly enhanced in the presence of *Streptococcus mutans*, which

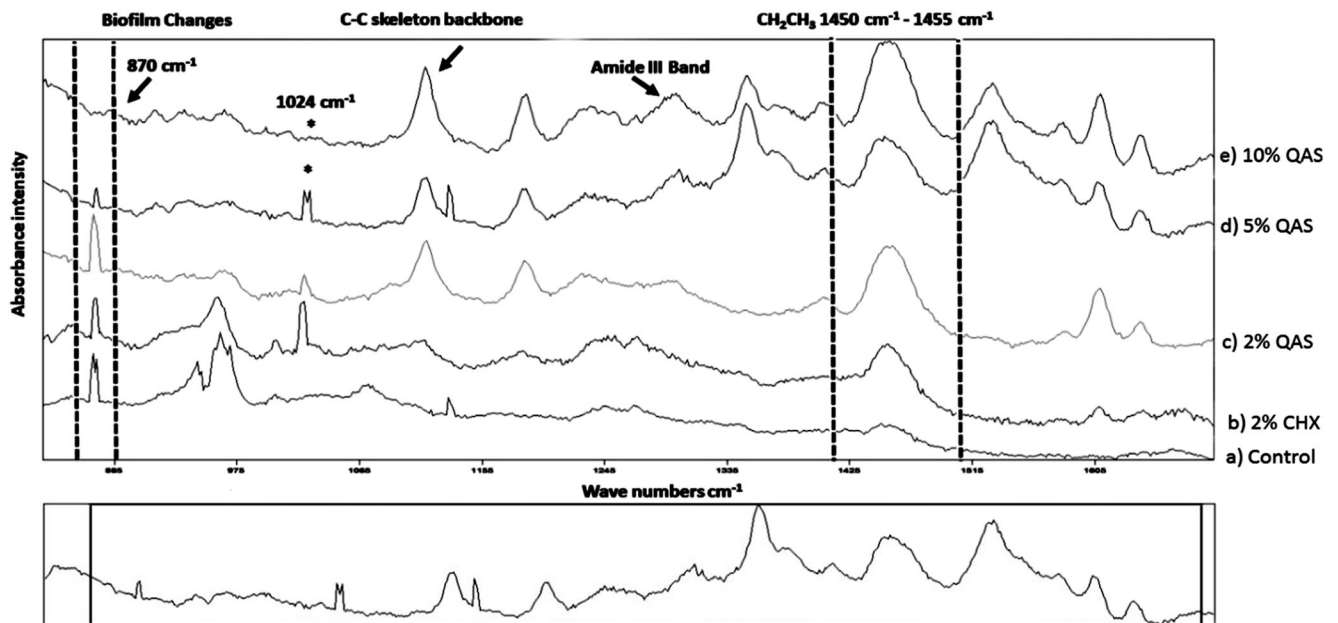


**Fig. 5** Raman spectra of dentine with treated biofilm cultivation. Dotted regions and arrowheads indicate the variation of peaks after treatment compared to control specimen without disinfectant treatment

**Table 4** Typical band assignments of Raman spectrum of dentin collagen disc specimens in both innate state and after QAS treatment of dentin disc specimens

Control	Assignment/vibrational mode	2% CHX	2% QAS	5% QAS	10% QAS	Ref
870 $\text{cm}^{-1}$	Single-bond stretching vibrations for amino acids proline and valine	871 $\text{cm}^{-1}$	865 $\text{cm}^{-1}$	866 $\text{cm}^{-1}$	867 $\text{cm}^{-1}$	30
1024 $\text{cm}^{-1}$	Carbohydrates	1021 $\text{cm}^{-1}$	1022 $\text{cm}^{-1}$	1023 $\text{cm}^{-1}$	1019 $\text{cm}^{-1}$	31
1128 $\text{cm}^{-1}$	C–C str, C–O–C glycosidic link	1128 $\text{cm}^{-1}$	1124 $\text{cm}^{-1}$	1121 $\text{cm}^{-1}$	1119 $\text{cm}^{-1}$	32
1450 $\text{cm}^{-1}$	C–H alkyl group	1453 $\text{cm}^{-1}$	1457 $\text{cm}^{-1}$	1460 $\text{cm}^{-1}$	1462 $\text{cm}^{-1}$	27, 28
1246 $\text{cm}^{-1}$	Amide III/C–N stretch; N–H; peptide carbonyl	1245 $\text{cm}^{-1}$	1249 $\text{cm}^{-1}$	1255 $\text{cm}^{-1}$	1261 $\text{cm}^{-1}$	27, 28
1665 $\text{cm}^{-1}$	Amide I/N–H inplane deformation alpha helix	1665 $\text{cm}^{-1}$	1658 $\text{cm}^{-1}$	1656 $\text{cm}^{-1}$	1653 $\text{cm}^{-1}$	27, 28

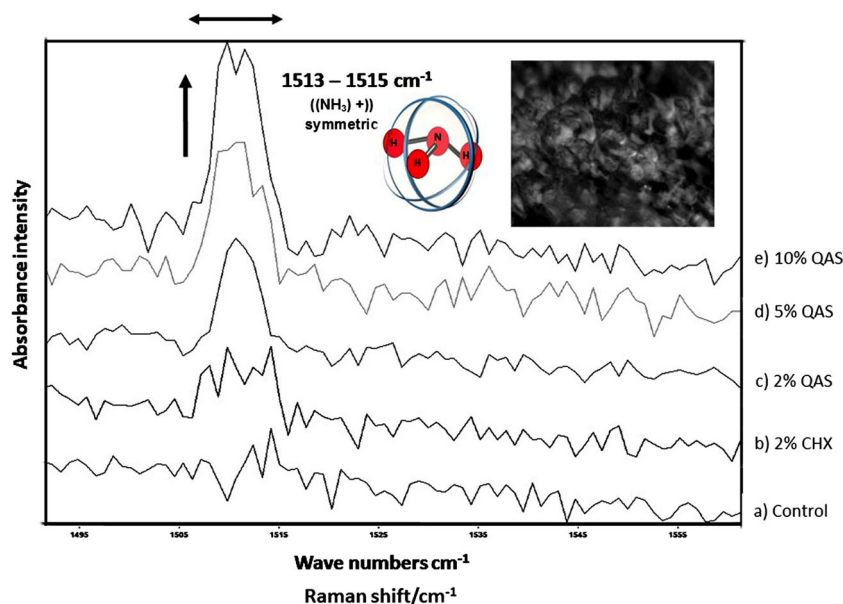
create the necessary niche capable of mechanically retaining the *Lactobacilli* [49]. When compared to mono-species biofilms, the dual-species biofilm includes the interaction between two species and provides a means for studying more complex microbial ecosystems. However, it is different from the in vivo multi-species plaque biofilms in both survival and pathogenic potential. Therefore, the results cannot be extrapolated to the in vivo situation and caution should be exercised in their interpretation.

In addition, CLSM, CFU counts, and MTT assay were used to evaluate bactericidal effects of CHX and QAS. The CLSM analysis revealed green and red fluorescence intensities within the single- and dual-species biofilms. The red fluorescence is a consequence of SYTO9 emission bands within the red wavelength [50]. Most of the bacteria present in the biofilm fluoresced green in the control group, indicating that the bacteria were mostly alive in the control, while the majority of the bacteria present in both the single- and dual-species biofilms fluoresced red in the CHX and QAS groups. Furthermore, a moderate decrease in MTT activities and bacterial viability was observed following treatment with CHX and QAS; hence,

the first null hypothesis that QAS had no antimicrobial effect on single-species and dual-species biofilms has to be rejected. Thus, in the current study, the results indicated the antimicrobial effectiveness of 2% QAS as the minimal concentration to achieve the desired efficacy when compared to higher concentrations and hence could have overcome any shortcomings of existing disinfectants, as per our previous studies.

Most of the attention regarding caries are given to the use of CHX when dealing with antimicrobials. The effect of CHX has been seen to reduce bacterial load, carious pathogens, demineralization of enamel, and acid production seen in case of biofilms. Although there was a caries inhibiting outcome of 46%, a meta-analysis of effects of CHX showed variable outcomes reporting differences when compared to fluoride varnish [51]. Other analysis suggested an insignificant, variable outcome and effect on the inhibition of caries [52]. CHX is water-soluble and can also leach out from the bonded interfaces, resulting in loss of antimicrobial and protease inhibitory activities. The original gluconate salt form of CHX, a *biguanide* compound, is considered a strong base and is relatively poorly soluble in water [53]. It has been replaced by

**Fig. 6** Raman spectra of dentine specimens grown with multi-species biofilm and treatment with different concentrations of QAS and CHX disinfectants. Arrow regions show the change in 1513–1515  $\text{cm}^{-1}$  wave region with peak-based discrimination



chlorhexidine digluconate. In order to design QAS with enhanced antimicrobial properties, an ethoxylated version of the QAS, which has been tested effective against *Porphyromonas gingivalis* and *Enterococcus faecalis*, was used [54]. The sol-gel synthesis provides a facile method for synthesizing organosilicates under mild conditions. The use of a tetrafunctional organosilane as the anchoring unit for the antimicrobial trialkoxysilane molecules enables a three-dimensional network to be formed once condensation is brought to completion within the dentinal substrate [55]. This minimizes the possibility for individual Et-SiQAC molecules to leach out of the bonded interface and provides considerably longer antimicrobial activity. Because of the presence of reactive silanol groups generated during hydrolysis, QAS can covalently attach to substrate surfaces via Si–O linkages to exert non-migrating microbiocidal functions [22]. As a result of their surfactant properties, QAS forms a protective antimicrobial film after reacting with the surface of materials. This surfactant activity may result in reduction of microbial adherence to circumvent or slow down biofilm formation [56].

QAS has strong broad-spectrum antibacterial properties. It is not required to enter the bacterial cell due to the interference of the ion transport and membrane lysis [14]. The positively charged quaternary group,  $N^+$ , within the pyridinium ring, has a high affinity for the negatively charged bacterial cell membrane, resulting in a massive discrepancy of the ionic balance and bursting of the bacterium under its own osmotic pressure. Due to the presence of long-chain lipophilic alkyl chains, the action of quaternary ammonium compounds against microbes is strong and rapid [57]. Furthermore, QAS also inhibits matrix-bound metalloproteinases and cathepsins that are responsible for degradation of demineralized collagen fibrils at the resin-dentine bonded interfaces [25].

Spectroscopic techniques such as Raman spectroscopy have been used for identification and study of bacterial components within the microbial mass and the biofilm structure, also offering easier sample preparation and additional benefits of molecular-level information [58]. In particular, Raman spectra as well as the maximum intensity projections seen in the region of  $480\text{--}490\text{ cm}^{-1}$  could be assigned to polysaccharides or carbohydrates [37, 59, 60]. The obtained spectrum contains multidimensional information on the presence of some cellular components. However, it seems that the different concentrations of QAS and 2% CHX used have resulted in deviations and marked differences in the intensity of the Raman spectra as a result of variations in structural elements. In the 7-day biofilms, treated and untreated with disinfectants, the control specimens showed intensive signals at the region of  $484\text{ cm}^{-1}$ . Additionally, the Raman signals assigned to these polysaccharides were also detected in other samples treated with different concentrations of QAS and 2% CHX. Based on the comparability of different spectra, 10% QAS specimens showed the least amount of intensity, followed by

5% QAS, 2% QAS, and 2% CHX. These accompanying Raman bands are spectroscopic signatures of carbohydrates within the biofilm as the peak appears more dull and broad, hypothesizing that more bacterial colonies are being affected at higher concentrations of QAS.

This study demonstrates that the viability of biofilms is affected by the QAS used. Interestingly, oral bacteria, such as *S. mutans*, colonize and form tooth surface biofilms and metabolize carbohydrates to produce organic acids. This results in dental caries formation specifically at the tooth restoration interface. The QAS compounds alter the surface electrostatic balance of the bacterial cells [61], resulting in a massive leakage within the cellular wall. With QAS concentration increasing from 2 to 10% (Fig. 4), there is a decrease in the Raman intensity of the  $484\text{ cm}^{-1}$  region as the peak appears more dull and broad, hypothesizing that more bacterial colonies are being affected. Hence, the second null hypothesis that QAS cavity cleanser had no effect on the multi-species biofilm can be rejected. In accordance with the results of the current study, QAS have promising antibacterial potential and can be further explored as cavity disinfectants prior to the application of self-etch or etch-and-rinse dental adhesives.

The Raman spectrum in Fig. 5 showed differences in the peaks of  $\text{CH}_2\text{CH}_3$ , amide I, and amide III among the 2%, 5%, and 10% QAS groups. The interaction of QAS with demineralized dentine may have resulted in a chemical modification of the tooth structure after elimination of bacterial colonies. Hence, the third null hypothesis that the QAS cavity disinfectants had no effect on demineralized dentine collagen matrix has to be rejected. The amide I, III, and the C–H alkyl group ( $1450\text{ cm}^{-1}$ ) show shifts with higher frequencies as the concentration of the QAS within the disinfectants increased from 2 to 10% (Table 4). The observed shifts may be due to sensitivity of the polypeptide chain [62], as these regions are responsive to most common spectral changes as a result of secondary structure of the polypeptide chain [63]. This may have contributed to the observed shifts and sharpening or broadening of the peaks. However, the mechanisms of chemical structure improvements within the dentine structure should be understood with the interplay among the microstructural components. The amide bands (I and III) are generally employed to study the protein structure showing visible excitation, which are more responsive within the specimens from the 2%, 5%, and 10% QAS groups, suggesting a stable three-dimensional structure with interchain hydrogen bonds [64]. The exact mechanism of this reinforcement needs further exploration on biofilms and changes within the amide and C–H alkyl regions. Moreover, the result corroborated with the emergence of peaks at  $1513\text{--}1515\text{ cm}^{-1}$  in some of the specimens, where the spectral peaks changed and became well-formed peaks dominating in 2%, 5%, and 10% QAS groups (Fig. 6). The CHX-treated specimens showed lesser intensity at the same region (Fig. 6). The peak may be erroneously

amounted to amide II region as it occurs in the vicinity of the 1515–1530  $\text{cm}^{-1}$  region [65]. Because of an increase in the height of the peaks, it was concluded that the random coils and turns of proteins were maintained [66].

## Conclusion

Under the experimental conditions of this *in vitro* study, it is possible to conclude that the use of quaternary ammonium silane disinfectants is effective and has contributed in ensuring a significant decrease in microbial growth of biofilms. This antibacterial effect also correlated with the changes in Raman vibrations specific to the concentration of QAS used. The treatment of acid-etched dentine with 2% QAS cavity disinfectant for 20 s has antimicrobial efficacy ensuring a significant decrease in microbial growth of biofilms. The underlying results related to antimicrobial action by 2% QAS against bacterial growth show strong potential for development of safer disinfectants in adhesive dentistry.

**Acknowledgements** The authors thank the labs at Microbiology HKU for the research experiments and analysis. Quaternary ammonium silane cavity disinfectant used in this study was generously supplied by KHG fiteBac Technology, Marietta, GA, USA.

**Funding** The work was supported by the Department of Paediatric Dentistry and Orthodontics, Faculty of Dentistry, The University of Hong Kong, Prince Philip Dental Hospital.

## Compliance with ethical standards

**Conflict of interest** The authors declare that they have no conflict of interest.

**Ethical approval** This article does not contain any studies with human participants or animals performed by any of the authors.

**Informed consent** For this type of *in vitro* study, formal consent was not required.

## References

- Paddick JS, Brailsford SR, Kidd EAM, Beighton D (2005) Phenotypic and genotypic selection of microbiota surviving under dental restorations. *Appl Environ Microbiol* 71:2467–2472
- Bammann LL, Estrela C (2009) Microbiological aspects in endodontics. *Endodontic Science (Edition 2)* 1:258–281
- Marsh PD (2003) Are dental diseases examples of ecological catastrophes? *Micro* 149:279–294
- Klein MI, Hwang G, Santos PHS (2015) Streptococcus mutans-derived extracellular matrix in cariogenic oral biofilms. *Front Cell Infect Microbiol* 33:5–10
- Bowen WH, Koo H (2011) Biology of Streptococcus mutans derived glucosyltransferases: role in extracellular matrix formation of cariogenic biofilms. *Caries Res* 45:69–86
- Hojo K, Nagaoka S, Ohshima T (2009) Bacterial interactions in dental biofilm development. *J Dent Res* 88:982–990
- Takahashi N, Nyvad B (2011) The role of bacteria in the caries process: ecological perspectives. *J Dent Res* 90:294–303
- Shi S, Zhao Y, Hayashi Y, Yakushiji M, Machida Y (1999) A study of the relationship between caries activity and the status of dental caries: application of the Dentocult LB method. *Chin J Dent Res* 2: 34–37
- Milnes AR, Bowden GH, Hamilton IR (1985) Effect of NaF and pH on the growth and glycolytic rate of recently isolated strains of oral Lactobacillus species. *J Dent Res* 64:401–404
- Loesche WJ, Eklund S, Earnest R, Burt B (1984) Longitudinal investigation of bacteriology of human fissure decay: epidemiological studies in molars shortly after eruption. *Infect Immun* 46:765–772
- Badet MC, Richard B, Dorignac G (2001) An *in vitro* study of the pH lowering potential of salivary lactobacilli associated with dental caries. *J Appl Microbiol* 90:1015–1018
- Simecek JW, Diefenderfer KE, Cohen ME (2009) An evaluation of replacement rates for posterior resin-based composite and amalgam restorations in US Navy and Marine Corps recruits. *J Am Dent Assoc* 140:200–209
- Donmez N, Belli S, Pashley DH, Tay FR (2005) Ultrastructural correlates of *in vivo/in vitro* bond degradation in self-etch adhesives. *J Dent Res* 84:355–359
- Spencer P, Ye Q, Misra A, Goncalves SEP, Laurence JS (2014) Proteins, pathogens and failure at the composite-tooth interface. *J Dent Res* 93:1243–1249
- Marsh PD, Martin M (2009) *Oral microbiology*, 5th edn. Churchill; Livingstone, Oxford
- Van Strydonck DA, Timmerman MF, van der Velden U, Weijden GA (2005) Plaque inhibition of two commercially available chlorhexidine mouthrinses. *J Clin Periodontol* 32:305–309
- Hebling J, Pashley DH, Tjäderhane L, Tay FR (2005) Chlorhexidine arrests subclinical degradation of dentin hybrid layers *in vivo*. *J Dent Res* 84:741–746
- Scaffa PM, Vidal CMP, Barros N, Gesteria TF, Carmona AK, Breschi L, Pashley DH, Tjaderhane L, Carillho MR (2012) Chlorhexidine inhibits the activity of dental cysteine cathepsins. *J Dent Res* 91:420–425
- Sadek FT, Braga RR, Muench A, Liu Y, Pashley DH, Tay FR (2010) Ethanol wet-bonding challenges current anti-degradation strategy. *J Dent Res* 89:1499–1504
- Tischer M, Pradel G, Ohlsen K, Holzgrabe U (2012) Quaternary ammonium salts and their antimicrobial potential: targets or non-specific interactions? *Chem Med Chem* 7:22–31
- Yuen JWM, Yung JYK (2013) Medical implications of antimicrobial coating polymers—organosilicon quaternary ammonium chloride. *Mod Chem Appl* 1:107
- Isquith AJ, Abbott EA, Walters PA (1972) Surface-bonded antimicrobial activity of an organosilicon quaternary ammonium chloride. *Appl Micro* 24:859–863
- Harkes G, Dankert J, Feijen J (1992) Growth of uropathogenic E. coli strains at solid surfaces. *J Biomater Sci Polym Ed* 3:403–418
- Jawetz E, Melnick JL, Adelberg EA, Brooks GF, Butel JS, Ornston LN (1989) *Medical microbiology*. Prentice-Hall, London, p 46
- Thompson RA, Allenmark S (1989) Effects of molecular association on the rates of hydrolysis of long chain alkyl betainates (alkoxycarbonyl-N, N,N-trialkylmethanaminium halides). *Acta Chem Scand* 43:690–693
- Zhang W, Luo XJ, Niu LN, Liu SY, Zhu WC, Epasinghe J (2014) One-pot synthesis of antibacterial monomers with dual biocidal modes. *J Dent* 42:1078–1095
- Gong SQ, Epasinghe DJ, Zhang W, Zhou B, Niu LN (2014) Synthesis of antimicrobial silsesquioxane–silica hybrids by hydrolytic co-condensation of alkoxy silanes. *Polym Chem* 5:454–462

28. Ivnitski D, Abdel-Hamid I, Atanasov P, Wilkins E (1999) Biosensors for detection of pathogenic bacteria. *Biosens Bioelectron* 14:599–624
29. Naumann D Infrared spectroscopy in microbiology. In: Meyers RA (ed) *Encyclopedia of analytical chemistry*. John Wiley & Sons, Ltd., Chichester, pp 102–131
30. Daood U, Yiu CKY, Burrow MF, Niu LN, Tay FR (2017) Effect of a novel quaternary ammonium silane cavity disinfectant on durability of resin-dentine bond. *J Dent* 60:77–86
31. Daood D, Yiu CKY, Burrow MF, Niu LN, Tay FR (2017) Effect of a novel quaternary ammonium silane on dentine protease activities. *J Dent* 60:77–86
32. Machado LF, Gonzalez Lopez S, Gonzalez Rodriguez MP (2004) Decalcification of root canal dentine by citric acid, EDTA and sodium citrate. *Int Endo J* 37:365–369
33. Xiao J, Klein MI, Falsetta ML, Lu B, Delahunty CM (2012) The exopolysaccharide matrix modulates the interaction between 3D architecture and virulence of a mixed-species oral biofilm. *PLoS Pathog* 8:e1002623
34. Ikeda T, Sandham HJ, Bradley EL Jr (1973) Changes in *Streptococcus mutans* and lactobacilli in plaque in relation to the initiation of dental caries in Negro children. *Arch Oral Biol* 18: 555–566
35. Soares LE, do Espirito Santo AM, Junior AB, Zanin FA, da Silva Carvalho C, de Oliveira R, Martin A (2009) Effects of Er:YAG laser irradiation and manipulation treatments on dentin components, part 1: Fourier transform-Raman study. *J Biomed Opt* 14:1–7
36. Alebrahim MA, Krafft C, Popp J (2015) Raman imaging to study structural and chemical features of the dentin enamel junction. *Mater Sci Eng* 92:1–9
37. Schuster KC, Reese I, Urlaub E, Gapes JR, Lendl B (2000) Multidimensional information on the chemical composition of single bacterial cells by confocal Raman microspectroscopy. *Anal Chem* 72:5529–5534
38. Ramakrishnaiah R, Rehman G, Basavarajappa S, Al Kkhuraif AA, Durgesh BH, Khan AS, Rehman I (2015) Applications of Raman spectroscopy in dentistry: analysis of tooth structure. *App Spect Rev* 50:332–350
39. Silva Júnior ZS, Botta SB, Ana PA, França CM, Fernandes KP, Ferrari RA, Mesquita-Ferrari RA, Deana A, Kalil Bussadori SK (2015) Effect of papain-based gel on type I collagen—spectroscopy applied for microstructural analysis. *Sci Rep* 5:11448
40. Xu C, Wang Y (2011) Cross-linked demineralized dentin maintains its mechanical stability when challenged by bacterial collagenase. *J Biomed Mater Res B Appl Biomater* 96:242–248
41. Kengne-Momo RP, Daniel P, Lagarde F, Jeyachandran YL, Pilard JF, Durand-Thouand MJ, Thouand G (2012) Protein interactions investigated by the Raman spectroscopy for biosensor applications. *Int J Spect ID* 46290
42. Rehman I, Smith R, Hench LL, Bonfield W (1995) Structural evaluation of human and sheep bone and comparison with synthetic hydroxyapatite by FT-Raman spectroscopy. *J Biomed Mater Res* 29:1287–1294
43. Cheng WT, Liu MT, Liu HN, Lin SY (2005) Micro-Raman spectroscopy used to identify and grade human skin pilomatrixoma. *Micro Res Tech* 68:75–79
44. Dukor RK (2002) Vibrational spectroscopy in the detection of cancer. *Biomed Appl* 5:3335–3359
45. Notingher I, Green C, Dyer C (2004) Discrimination between ricin and sulphur mustard toxicity in vitro using Raman spectroscopy. *J Roy Soc Interfac* 1:79–90
46. Ferracane JL (2013) Resin-based composite performance: are there some things we can't predict? *Dent Mater* 29:51–58
47. Nyvad B, Kilian M (1987) Microbiology of the early colonization of human enamel and root surfaces in vivo. *Scand J Dent Res* 95: 369–380
48. Banas JA (2004) Virulence properties of *Streptococcus mutans*. *Front Biosci* 9:1267–1277
49. Caufield PW, Schön CN, Saraithong P, Li Y, Argimón S (2015) Oral lactobacilli and dental caries: a model for niche adaptation in humans. *J Dent Res* 94(9 Suppl):110S–118S
50. Stocks SM (2004) Mechanism and use of the commercially available viability stain. *BacLight Cytometry A* 61:189–195
51. Baca P, M'ou, Bravo M, Junco P, Baca AP (2002) Effectiveness of chlorhexidine–thymol varnish (Cervitec) for caries reduction in permanent first molars of 6–7-year-old children. 24-month clinical trial. *Community Dent Oral Epidemiol* 30:363–368
52. Twetman S, Stecksén-Blicks C (2008) Probiotics and oral health effects in children. *Int J Paediatr Dent* 18:3–10
53. Foulkes DM (1973) Some toxicological observations in chlorhexidine. *J Periodontol Res Suppl* 12:55–60
54. Meghil MM, Rueggeberg F, El-Awady A, Miles B, Tay F, Pashley D, Cutler CW (2015) Novel coating of surgical suture confers antimicrobial activity against *Porphyromonas gingivalis* and *Enterococcus faecalis*. *J Periodontol* 86:788–794
55. Liu Y, Xu D, Wu Y, Sun H, Gao H (2004) Comparative study on the hydrolysis kinetics of substituted ethoxysilanes by liquid-state <sup>29</sup>Si NMR. *J Non-Cryst Solids* 343:61–70
56. Kugel A, Staflieni S, Chisholm BJ (2011) Antimicrobial coatings produced by “tethering” biocides to the coating matrix: a comprehensive review. *Prog Org Coat* 72:222–252
57. Devinsky F, Masarova L, Lacko I, Mlynarcik D (1991) Structure activity relationships of soft quaternary ammonium amphiphiles. *Aust J Biol Sci* 2:1–10
58. Efrima S, Zeiri L (2008) Understanding SERS of bacteria. *J Ram Spect* 40:277–288
59. Gałat A (1980) Study of the Raman scattering and infrared absorption spectra of branched polysaccharides. *Acta Biochem Pol* 27: 135–142
60. Wiercigroch E, Szafranec E, Czamara K, Pacia MZ, Majzner K, Kochan K, Kaczor A, Baranska M, Malek K (2017) Raman and infrared spectroscopy of carbohydrates: a review. *Spectrochim Acta A Mol Biomol Spectrosc* 185:317–335
61. Beyth N, Yudovin-Farber I, Bahir R (2006) Antibacterial activity of dental composites containing quaternary ammonium polyethylenimine nanoparticles against *Streptococcus mutans*. *Biomaterials* 27:3995–4002
62. Gniadecka M, Nielsen OF, Wessel S, Heidenheim M, Christensen DH, Wulf HC (1998) Melanoma diagnosis by Raman spectroscopy and neural networks: structure alternations in proteins and lipids in intact cancer tissue. *J Invest Dermatol* 122:443–449
63. Diem M, Romeo M, White SB, Miljkovic M, Matthaus C (2004) A decade of vibrational micro-spectroscopy of human cells and tissue (1994–2004). *Analyst* 129:880–885
64. Pelton JT, Maclean LR (2000) Spectroscopic methods for analysis of protein secondary structure. *Anal Biochem* 277:167–176
65. Wang HY, Zhang YQ (2014) Processing and characterisation of a novel electropolymerized silk fibroin hydrogel membrane. *Sci Rep* 4:6182
66. Rehman IU, Movasaghi Z, Rehman Shezza (2012) CRC Press, Taylor and Francis Group. *Vibrational spectroscopy for tissue analysis*, pp 64–83. Series in Medical Physics and Biomedical Engineering

**Publisher's note** Springer Nature remains neutral with regard to jurisdictional claims in published maps and institutional affiliations.